2009

An improved synthesis of the HDAC inhibitor trichostatin A

Joseph Colombo

An Improved Synthesis of the HDAC Inhibitor Trichostatin A

by

Joseph Colombo

Thesis

Submitted to the Department of Chemistry

Eastern Michigan University

in partial fulfillment of the requirements for the degree of

MASTER OF SCIENCE

in

Chemistry

Thesis Committee:

Andrei Kornilov, PhD

Harriet Lindsay, PhD

Cory Emal, PhD

April 24, 2009

Ypsilanti, Michigan

Acknowledgements

I would like to thank my advisor and mentor, Dr. Andrei Kornilov, for introducing me to the research and development branch of organic chemistry and for his input and ideas on all of my research endeavors, as well as for letting me pursue my own ideas. I would also like to thank him for his flexibility in letting me complete graduate school. Thank you to Dr. Harriet Lindsay for being available to me for research advice and help in navigating the graduate school, as well as for her instructions in NMR analysis, which were quite valuable here. Thank you also to Dr. Cory Emal for his time and instruction. Thank you to Dr. Shawn Payne for being my on-call biologist to look over the sections that the chemists don't understand. I would also like to thank Cayman Chemical Company for their financial support.

Abstract

Histone deacetylase inhibitors (HDIs) have found a wide variety of medicinal uses and are most noted for their specific apoptotic action towards cancer cells. Several hydroxamate HDIs have since been moved on to phase 1 and 2 clinical drug trials, with one having already been approved for treatment of advanced cutaneous T-cell lymphoma. Trichostatin A is one of the most potent known naturally-occurring inhibitors of histone deacetylase. Unfortunately for researchers, the syntheses that have been reported are both long and difficult, which leads to a low overall yield and therefore to a prohibitively expensive product, limiting its medicinal potential. This work builds on several previously published syntheses and shows a more efficient synthesis of Trichostatin A, which will make it more available for use in a variety of treatments.

Table of Contents

List of Figures

Chapter I: Introduction

I.1 Histone Deacetylase

Cellular DNA usually exists in a condensed form wrapped around histones. Histones are nuclear proteins that, due to the presence of multiple lysine and arginine amino acids, are positively charged. This positive charge allows them to bond strongly with the negatively charged DNA backbone. In the condensed form, DNA cannot be transcribed. Before DNA can be transcribed, the histones are acetylated, neutralizing the positive charge and therefore weakening the histone-DNA bond. After transcription, these acetyl groups are removed so that the DNA can again condense on the histone.

Histone deacetylases (HDAC) are a group of enzymes that removes acetyl groups from the lysine residues on a histone. Removal of the acetyl groups, known as hypoacetylation, restores the normal positive charge to the histone and therefore allows the DNA to condense and prevents transcription (1→2, Figure 1). This silencing can become permanent if the unprotected lysines are then methylated (2→3, Figure 1). HDAC performs the reverse process of histone acetyltransferase (HAT), which transfers acetyl groups from acetyl CoA to the lysines on the histone, inducing a state known as hyperacetylation (2→1, Figure 1). Hyperacetylation causes a decreased binding of the histones to DNA and leads to chromatin expansion, allowing transcription to take place. Hyperacetylation of histones, which can be induced with various agents, increases the access of some transcription factors to nucleosomes, thereby increasing RNA transcription. Histone deacetylase inhibitors (HDI) lead to hyperacetylation by blocking the function of histone deacetylase, therefore leaving the lysine amino acids acetylated from the histone acetyltransferase and ultimately increasing

transcription. This process increases the amount of RNA present in the cell and their respective encoded proteins.

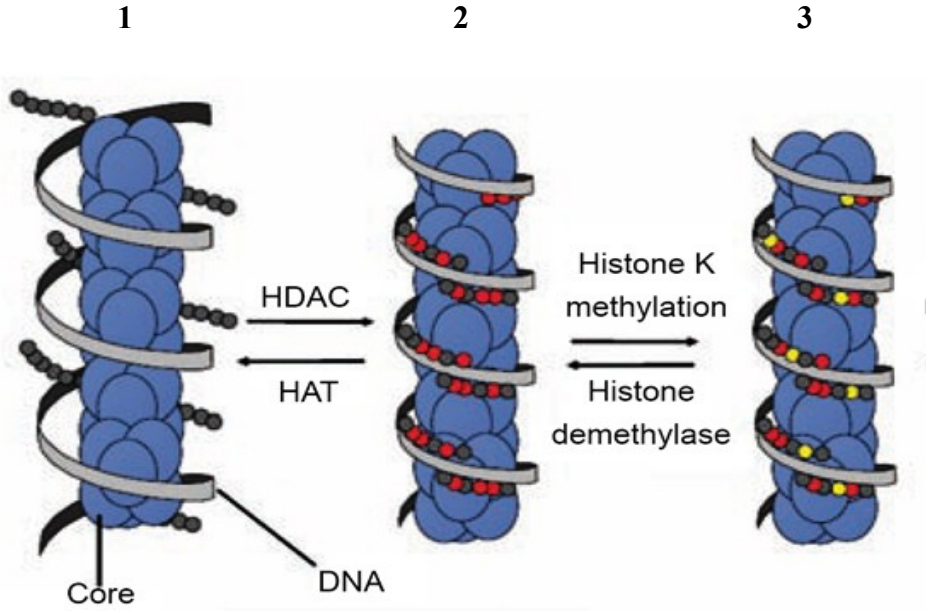

Figure 1. Transcriptional Inactivation [1]

HDACs can be categorized into several groups based on various factors, including their size, location, number of active sites, and homology to yeast HDAC proteins [2]. Class I HDACs, which are found in the nucleus, include HDAC1, HDAC2, HDAC3, and HDAC8, although HDAC3 has also been found in the cytoplasm [3]. Class II HDACs, which can shuttle into and out of the nucleus [3], consist of two different types, called IIa and IIb [2]. Those belonging to class IIa include HDAC4, HDAC5, HDAC7, and HDAC9 and contain a single catalytic active site. Those belonging to class IIb include HDAC6 and HDAC10, which contain two active sites [4]. Both class I and II HDACs function via a metal ion-dependent mechanism containing both a zinc and an iron cofactor [5].

Class III HDAC proteins, on the other hand, are distinct in that they operate by a NAD^+-dependent mechanism [2]. These are referred to as sirtuins and are named SIRT1-7.

These are found in a variety of subcellular locations, including the mitochondria, nucleus, and cytosol [3]. However, class III HDACs have a different method of action compared to class I, II, and IV HDACs, and as such are not affected by most HDIs.

Class IV HDACs, the most recently discovered class [6], contains only one protein, HDAC11. While this class is similar in tertiry structure to classes I and II, class IV HDAC expression is tissue dependent and is found only in the kidney, heart, brain, skeletal muscle, and testis. Its subcellular localization is similar to class I HDACs, as it is only found within the cell nucleus. Like classes I and II, class IV HDACs operate by a metal ion-dependent mechanism.

I.2 Trichostatin A and Other Histone Deacetylase Inhibitors

Trichostatin A (TSA, Figure 2), a hydroxamic acid, was the first naturally occuring HDI to be discovered. It is also one of the most potent HDIs, and, as such, is widely used in experimentation. Initially reported in 1976, TSA was first discovered as an antifungal antibiotic isolated from a culture broth of *Streptomyces platensis* [7]. It was not until 1987 that its anti-proliferative activity was discovered, though its mechanism of action was not known [8].

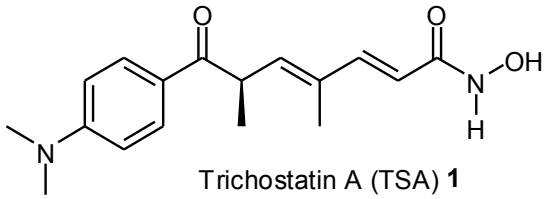

Trichostatin A (TSA) **1**

Figure 2. TSA

In 1990 it was found that TSA caused an increase in acetylated histones in a variety of mammalian tumor cell lines [9]. TSA was shown to be a selective histone deacetylase inhibitor, reversibly inhibiting classes I, II and IV types of HDAC while not affecting class

III. Figure 3 shows TSA bound to class I HDAC 8.

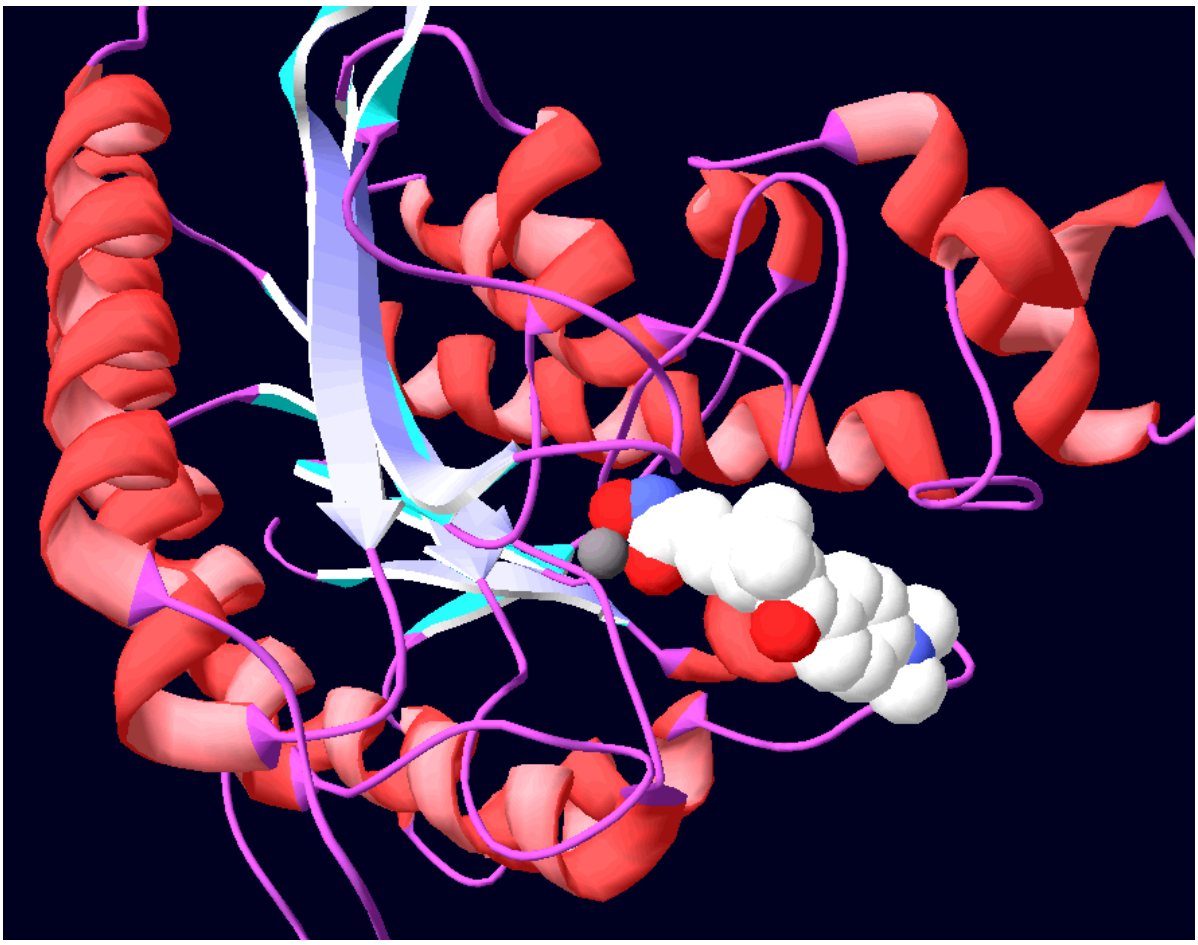

Figure 3. TSA Bound to HDAC8, as represented by the PDB

TSA, which exhibits an IC_{50} in the nanomolar range against class I, II, and IV HDACs [10], contains an aliphatic chain that occupies a tubular pocket in the target HDAC enzyme and functions as an HDI by chelating to the zinc atom at the bottom of this pocket in the HDAC protein, displacing the cation (Figure 4) [11]. This reversible inhibition enables a greater amount of transcription within the cell.

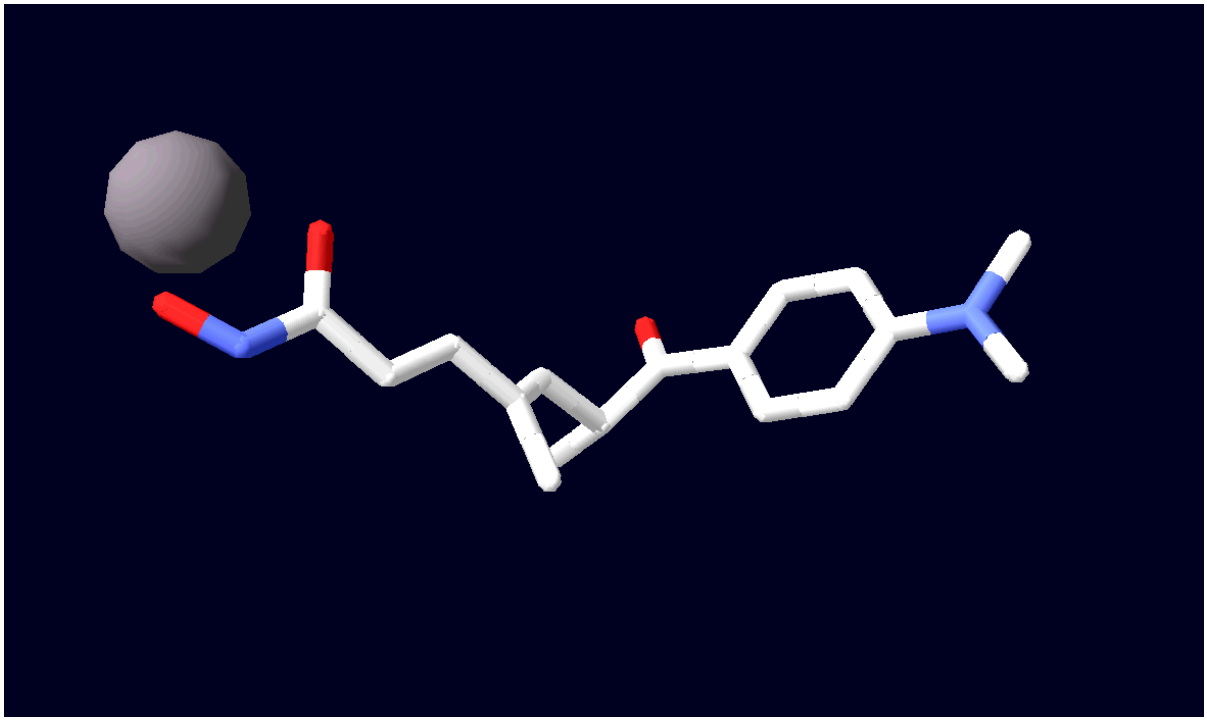

Figure 4. TSA Bound to Zinc

TSA is most often used in HDAC experiments because it is typically found to be the most potent of the HDIs [12]. It has been found to be 3 to 30 times more potent (depending on the specific cell line) than another popular HDI, suberoylanilide hydroxamic acid (SAHA, Figure 5). Due to its ease of synthesis, SAHA is another of the most commonly used HDIs in investigations. SAHA, also known by the commercial name of Vorinostat, interacts with HDAC via the same method as TSA and has recently been approved by the FDA for use in treatment of advanced cutaneous T-cell lymphoma [13]. TSA has not been examined for use as a commercial drug due to the long synthesis and high manufacturing cost, issues the work described here addresses.

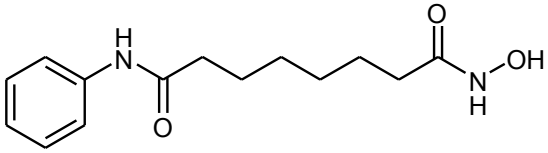

Suberolanilide Hydroxamic Acid (SAHA) **2**

Figure 5. SAHA

A variety of other HDIs are used for various research purposes, several of which are in various stages of clinical trials as anticancer agents [14]. PCI-24781, produced by Pharmacyclics, and LBH 589, produced by Novartis, are both in Phase I clinical trials (Figure 6). PXD 101, produced by CuraGen, is currently in Phase II clinical trials for treatment of ovarian cancer. Like SAHA and TSA, these compound all contain an aromatic unit separated from the hydroxamic acid group by a hydrocarbon chain. As with their naturally occurring cousins, the hydroxamic acid group binds with the zinc cofactor in type I, II, and IV HDACs while the chain and bulky aromatic group block access to the pocket of the protein, halting the deacetylation ability of the protein [15].

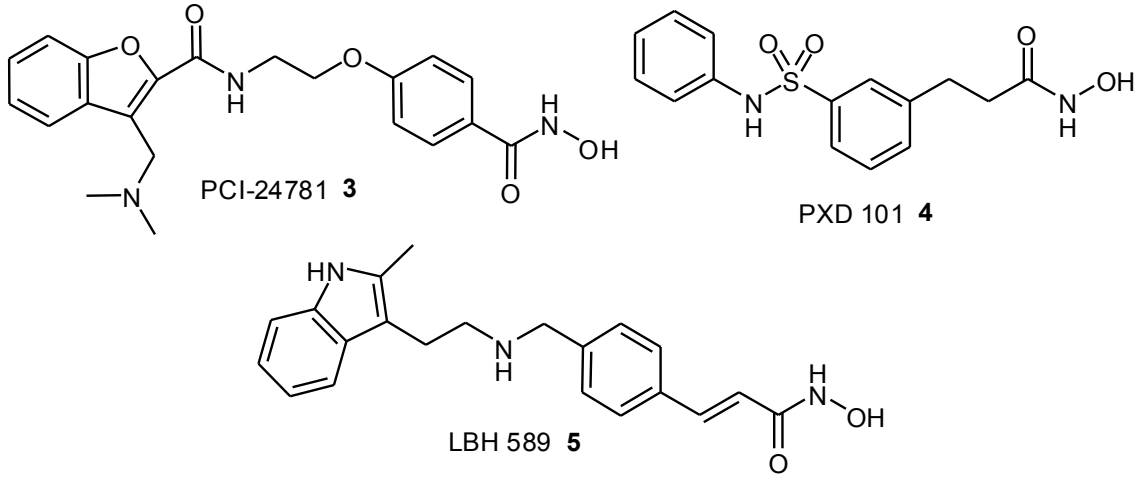

PCI-24781 **3**

PXD 101 **4**

LBH 589 **5**

Figure 6. Several Hydroxamate HDIs currently in Clinical Trials

Another reversible HDAC inhibitor commonly used due to its simple structure and synthesis is sodium butyrate, which has a significantly different structure than the other HDIs

discussed here (Figure 7). Sodium butyrate has an effective dose that is more than four orders of magnitude greater than TSA (5 mM vs 0.3 μM) [16]. However, it is also effective against class III HDACs [17]; this shows that it operates through a different method of action than the other HDIs discussed here.

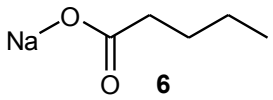

6

Figure 7. Sodium Butyrate

I.3 Use of TSA in Cancer Treatment

One of the most important applications of HDIs in general and of TSA in particular is cancer treatment. A precise control of the normal cell cycle progression is extremely important for the homeostasis of normal tissue cells. Accordingly, the cell has developed multiple controls at various stages of the cell cycle. Failure of cell cycle regulation may be caused by several different factors, including mutations in tumor suppressor genes or proto-oncogenes controlling these checkpoints, or by altered expression or activity of cyclin-dependent kinases (CDKs). In these cases, cells undergo unrestricted cell proliferation, resulting in tumorigenesis [18].

Class I and II HDAC proteins have been observed to be overexpressed in certain types of cancer, with HDAC1-3 being overexpressed in ovarian cancer [19], HDAC2 overexpressed in gastric cancer [20], HDAC1 and 3 overexpressed in lung cancer [21], and aberrant expression of HDAC6 in some breast cancers [22]. In addition, a possible correlation between acute myeloid leukemia and HDAC8 overexpression has been suggested [23].

There are various paths of possible chemical intervention in cancer based on targeting important cell cycle moderators. They include inhibitors of CDK activity, protein kinase c

inhibitors, proteasome inhibitors, farnesyl transferase inhibitors, inhibitors of tyrosine kinase receptors, FRAP-mTOR/p70S6k inhibitors, and antiangiogenic compounds [24]. However, these chemotherapeutic agents act on basic mechanisms of cell proliferation and are not tumor cell type specific. As a result, considerable toxicity occurs in normal cells, specifically those with a high turnover or proliferation rate, such as those in the intestinal epithelia, male germ cells, skin, hair follicles, and the hematopoietic system [18]. It is this problem that leads to the common chemotherapy side-effects of nausea and vomiting, impotence, skin discoloration, loss of hair, and immunosuppression [24].

While these treatments are often successful, researchers are attempting to find a new class of drug that avoids the variety of side effects caused by lack of specificity. With improved understanding of the molecular mechanisms involved in tumor suppressor, onco-genes, and cancer cells, a promising new area of investigation is emerging in the development of new, anticancer compounds that exhibit improved tumor selectivity [18]. As a result of this increased selectivity, the new compounds exhibit lower toxicity than previous cancer treatments. As HDACs play an important role in the regulation of gene transcription and are involved in key biological processes including cell proliferation, differentiation, and survival, HDIs represent a promising new class of compounds that has gained considerable attention over the past few years. Indeed, increases in the activity levels of HDACs are often associated with tumor development. When an HDI such as TSA is introduced to cancer cells, it inhibits eukaryotic cell growth at the G1 and G2 stages of the cell cycle [25]. It is this inhibitory aspect of Trichostatin A and other HDIs that has been of most interest to researchers.

HDAC inhibitors disturb the steady-state level of nucleosomal histone acetylation,

leading to hyperacetylation of specific chromatin regions and deregulated transcription of a very selective subset of genes, resulting in transcriptional activation of some genes and repression of others. While this process in not fully understood, it tends to result in either the arrest of the cell cycle in growth phases 1 or 2, differentiation of the tumor cells, or apoptosis of the cells in a wide range of cancer cell lines at very low concentrations, typically nanomolar to micromolar. More recently, potent *in vitro* and *in vivo* antimetastatic [26] (reduction in the transmittance of cancer throughout the body) and antiangiogenic [27] (reduction in the growth of new blood vessels needed by tumors to grow and metastasize) properties have also been ascribed to these compounds, which further underscores their usefulness for the treatment of solid tumors. This explains the exponentially growing efforts being made to develop potent and highly specific HDAC inhibitors with favorable pharmacokinetic and safety profiles.

Earlier theories stated that class I-specific inhibitors would be most effective in treating cancers, as it was believed that only the expression of class I HDACs were involved in carcinogenesis. However, recent research [12] shows that HDAC6, a type II HDAC, is important in several key cancer functions involving destabilization of the microtubulin assembly and aggresome function. If this hypothesis is correct, a pan-HDAC inhibitor, such as TSA, would prove to be more effective in treating cancer than a class I-specific inhibitor. While it was thought that a selective inhibitor would exhibit less toxicity than a pan-inhibitor due to a smaller range of targeted proteins, the results of several preclinical trials have shown that the toxicity of the selective inhibitor [28-30] is equivalent to that of the pan-inhibitor [31-33].

While HDI compounds such as TSA and SAHA would be expected to react strongly

with the liver, as it is a key target for many types of drug-induced toxicity, toxicological studies have found no detrimental effects in hepatic tissue (normal liver cells) when exposed to TSA in active concentrations for cancer cells. Early research initially showed problems, as Papeleu and Loyer found that noncytotoxic levels of TSA induced cell cycle arrest in early S phase [34-35], leading to a halt in cell proliferation and a loss of liver tissue regeneration. However, later research by Papeleu found a decrease in pro-apoptotic Bid [34], while Vanhaecke found an increase in the anti-apoptotic basil cell lymphoma protein Bcl_{xL} [36]. These factors, in addition to the minimization of apoptosis caused by the layout of the cells [36-37], lead to a TSA-caused delay in the onset of apoptosis in these cells, rather than the induction seen in tumor cells.

Interestingly enough, the same effect is not evident in hepatoma cells, the cancer cells of the liver. Due to an upregulation of p21 and a downregulation of cyclin A [38], treatment with TSA causes an accumulation of hepatoma cells in the g2/M phase, resulting in a halting of tumor growth [39]. Strangely enough, this inhibition of DNA synthesis is even more pronounced in rat hepatoma cell lines than in human lines [38], showing that test results in animals cannot always be generalized to other species. In addition, both rat and human hepatoma cells treated with TSA show an increase in caspase-3 activity, a key protein that plays a central role in the execution-phase of cell apoptosis [38]. This, coupled with a down-regulation of anti-apoptotic Bcl2 and an up-regulation of pro-apoptotic Bax, leads to an induction of apoptosis [38]. It is interesting to note that while the Bcl (Basal cell lymphoma) protein family increased its apoptotic activity in cancer cells exposed to TSA, it is decreased in non-cancer cells, showing the powerful differential effects of HDIs on cancer cells.

HDIs have also been examined and found effective in treating many other forms of

cancer. Glick *et al.* found that concentrations of m-carboxycinnamic acid bis-hydroxamide (CBHA, Figure 8) between 0.5 μM and 4.0 μM resulted in apoptosis in all of the nine neuroblastoma cell lines observed [40]. Schmidt and colleagues found that TSA exhibits cytocidal effects in MCF-7 breast cancer cells at concentrations of 100 nM, a 100-fold smaller concentration than that of the synthetic HDIs also examined [41]. Thaler *et al.* examined the effects of SAHA on a variety of prostate cancer cells [42]. They found that the growth of several cell lines (LNCaP, PC-3, and TSU-Pr1) was suppressed at micromolar concentrations (2.5 to 7.5 μM). In addition, they also found that treatment of SAHA at 50 mg/kg/day of mice transplanted with CWR22 tumors resulted in a 97% reduction of tumor size compared to the controls with no detectable toxicity. Zhu and colleagues examined the effects of TSA on lung cancer tissues both with and without a DNA methyltransferase inhibitor [43]. They observed that while a minimal dose (500 nM) of TSA exhibited a 93.5% cell viability, this viability decreased 57% for the same dose when the cells were pre-treated with the DNA methyltransferase inhibitor. In addition to these cancer lines, HDIs have also been used in treating ovarian cancer [19], gastric cancer [20], colorectal cancer [40, 44] and leukemia [45].

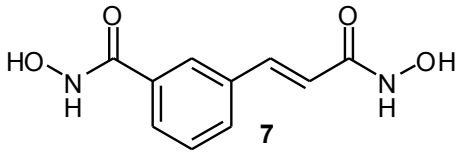

Figure 8. CBHA

One problem with using HDIs such as TSA for treatment of cancer is that while they cause apoptosis of the cancer cells, they also cause an increase of NF-κB, a transcription factor that inhibits apoptosis in all cell lines. NF-κB can be inhibited by proteasome inhibitors; several of these inhibitors, such as bortezomib and MG-132, have been studied in

breast cancer cell lines [10] but have shown only limited activity. However, Domingo-Domènech *et al.* [46] have shown a synergistic effect of these proteasome inhibitors when used in conjunction with a traditional HDI such as TSA or SAHA, due to an increased level of apoptosis evident in breast cancer cells. The combined treatment of these two compounds resulted in a decrease in cell viability of up to 50% over either compound alone. This synergistic effect is thought to be due to both a promotion of the stress-related pathways of the cell, as well as a disabling of the cytoprotective pathways. Given that both HDIs and proteasome inhibitors are in clinical trials, combinations of the two classes could be used as a new strategy for treatment of solid tumors.

While HDIs show a good deal of promise in treating a wide range of cancers, some research [47] indicates that HDIs may be not be potent enough to fully initiate apoptosis in some cancer lines on their own. However, treatment with TSA in conjunction with tumor necrosis factor-related apoptosis-inducing ligands (TRAIL) shows an increased apoptotic effect [48] that more than doubled the change in cell viability. Such techniques enable lower doses of the drugs to be used, minimizing the toxicity to the remainder of the body.

I.4 Use of TSA in Addiction Treatment

TSA has been studied in several different addiction processes, including alcohol and cocaine. Cocaine acts as a reuptake inhibitor of dopamine, serotonin, and norepinephrine. Cocaine addiction functions through several different neurological systems, including the general rewards system that is evident in most addictive behaviors, as well as through independent pathways that are still not completely understood.

Romieu *et al.* found TSA to be useful in decreasing self-administration of cocaine in a dose dependent manner [49]. Interestingly enough, this decrease was evident in cocaine, but

not evident in sucrose, a natural neurotransmitter reuptake inhibitor. This suggests specific interactions of HDACs and cocaine in the brain. This theory was further strengthened by the observation that HDAC activity in the frontal cortex of the brain was inhibited by administration of cocaine but not sucrose. A TSA dose of 0.3 mg/kg was also shown to result in a 40% decrease of total HDAC activity in the frontal cortex, a similar level to that induced by cocaine. Sucrose did not show an inhibition of HDAC activity in the frontal cortex, explaining the differences in effect of TSA between sucrose and cocaine administration. This suggests that TSA does not decrease cocaine administration by an inhibition of the general rewards system but by a process specific to cocaine's interaction with the brain. As such, HDIs can be used to decrease the reward sensation felt by cocaine without interfering with other reward systems in the brain. Use of TSA or another HDI can therefore avoid the general emotional numbing that is caused by anti-addiction drugs interacting with the general rewards pathway and specifically target the feelings caused by cocaine.

Excess consumption of alcohol, often due to alcohol addiction, or alcoholism, is a severe health threat and is one of the major health concerns of the industrialized world. Ethanol withdrawal symptoms, such as increased anxiety, risk of convulsions, and tremors, are some of the factors most needed to be managed when dealing with alcoholism [50]. Anxiety is a common early onset symptom of withdrawal. It often serves as a negative reinforcement for drinking, as anxiety is removed when more alcohol is consumed.

It has been shown in mouse models that acute alcohol exposure results in decreased HDAC activity and increased acetylation of H3 and H4 [50]. In contrast, the anxiety-like behaviors during chronic alcohol exposure withdrawal are associated with an increase in HDAC activity and decreases in acetylation of H3 and H4. When alcohol withdrawal was

mediated with TSA, it resulted in lowered levels of HDAC and an increase in acetylation of H3 and H4 compared to control groups. The anxiety of the studied mice was also decreased as shown by a threefold increase in time spent in a light environment, as well as a twofold increase in a response to an open-arm entrance test. These results suggest that HDAC inhibitors may be potential therapeutic agents in treating the anxiety associated with alcohol withdrawal symptoms.

I.5 Use of TSA in Neurological and Muscular Disorders

TSA has been studied in several different muscular and neurological disorders, including schizophrenia, multiple sclerosis, and spinal muscular atrophy. One current schizophrenia hypothesis states that the cause of the disorder is due to a lack of protein synthesis in the brain caused by the deacetylation of histone 3 by HDACs [51]. Studies on the neuronal cell lines have shown that TSA increases protein synthesis, allowing for more efficient gene regulation [52]. In addition, treatment with commercially available HDI on schizophrenic patients also found an increase in the acetylation of Lys9 and Lys14 of histone 3 [53]. Schizophrenics are characterized by a more "rigid" chromatin, meaning that the chromatin are more tightly bound and less able to translate RNA and transcribe proteins. It is thought that treatment with HDIs would relax the chromatin of schizophrenics, allowing for better gene regulation. This would then make the patients more likely to benefit from conventional treatment [54]. Alternately, researchers may someday be able to create specific chromatin remodeling agents that can directly target problem gene areas.

Multiple sclerosis (MS), first discovered in 1868 [55], is a demyelinating disease characterized by chronic inflammation of the central nervous system (CNS) white matter [2]. MS immunopathology is largely due to the cytotoxic action of myelin-specific pro-

inflammatory T cells on the CNS [56], although recent research suggests that humoral immune responses (antibodies produced by plasma cells) also play a significant role in the condition [57]. Studies have shown that HDAC levels were elevated in activated immune cells [58]. In addition, treatment with TSA activates a transcriptional program that culminates in decreased caspase 3 activation [59] and therefore has a dual function of suppressing the overactive immune system and depressing HDAC dependent programs that exacerbate the ongoing damage to the CNS.

Spinal muscular atrophy (SMA), the most common inherited disorder lethal to infants, is an autosomal-recessive motor neuron disease. The majority of those afflicted with SMA are not diagnosed until after they exhibit muscular weakness. SMA is caused by the deletion or mutation of survival motor neuron 1 (SMN1) while still maintaining a copy of SMN2 [60]. SMN1 produces full length SMN RNA and protein, but SMN2 typically produces mRNA that lacks an exon and produces an unstable protein, although a minority of the transcriptions produce functional SMN protein. It has been suggested that increasing protein production would result in longer and better lifespans for those afflicted with the condition. Avila and coworkers found that SMA-modified mice (mice modified to mimic protein production found in humans suffering from SMA) that were treated with TSA after motor defect was evident resulted in a higher weight and a 19% increase in lifespan over the control group, though the weights and lifespans were still less than that of wild type mice [61]. In addition, they also found an increase in the motor function of the SMA mice over the control group, which was evident before the changes in weight occurred.

I.6 Use of TSA in Cloning

In addition to treatment of existing conditions, treatment of embryos with HDIs such as TSA result in greater cloning efficiency. Somatic cell nuclear transfer (SCNT) is the process whereby the nucleus of a somatic cell is placed in an egg cell without a nucleus. It was first theorized that one of the reasons for low success rates in the use of SCNT in cloning is due to hypermethylation of the DNA of the somatic nucleus. Kishigami *et al.* found that treatment of zygotes with TSA resulted in a reduction of hypermethylation of the genome [62]. They later worked to optimize dose and timing of the inhibitor, which led to a two- to five-fold increase in success *in vitro* as defined by the number of cells that developed to blastocyst stage. They found that this technique worked in a wide variety of cells, including tail tip cells, spleen cells, neural stem cells, and cumulus cells, and, in some cell types, also increased the developmental rates. When tested *in vivo*, they found a six-fold increase in the number of successful somatic cell clones. Mice cloned in this manner were free of the deleterious phenotypes such as obesity or shortened lifespan that are usually associated with cloning. Li *et al.* later worked to optimize TSA amounts for cloning and managed to raise their odds of blastocyst formation from a 54% to an 80% success rate [63].

I.7 Summary

TSA has been found to be effective in the treatment of a wide variety of pathologies, including several addictions, schizophrenia, multiple sclerosis, and spinal muscular atrophy. TSA has also been found to be useful as a treatment in many types of cancers, where it acts specifically on the cancer tissue, leaving normal tissue unharmed. In addition, it has also been found useful in increasing the success rates of cloning attempts, both *in vitro* and *in vivo*. However, all of these treatments are problematic due to the difficulty in synthesizing TSA, which leads to a high cost of the compound. An improved synthesis would make TSA

more readily available to the research community for examination in a wide variety of applications.

Chapter II: Results and Discussion

Trichostatin A has been synthesized in several ways [8, 64-66], with the first synthesis published in 1983 [64]. Our work closely follows that published by Mori and Koseki [8]. There are several reasons this route was chosen, including an easily available starting material and the use of traditional chemical methods.

In our first attempt, we followed Mori and Koseki's original route through to completion with some small changes. While the first portion of their route worked well, the end of the route featured low yields and long reaction times. In order to improve it, we designed two alternate ways to finish the synthesis. While both of them reduced the synthesis time by more than a week, only the second improved the overall yield of the product. The results of our replication of the Mori and Koseki route as well as those of our two alternate approaches are defined herein.

The first portion of the synthesis is shown in Scheme 1. Protection of the commercially available hydroxy ester **8** with TBDMS-Cl gave silyl ester **9** in quantitative yield. The ester was then reduced with LiBH4 to yield alcohol **10** in a 76% yield along with a recovery of 16% of unreacted ester **9**. Oxidation of alcohol **10** under typical Swern conditions [67] gave aldehyde **11**, which was immediately treated with an aryl Grinard reagent to produce alcohol **12** in a 48% yield as a 1:1 mixture of diastereomers according to ^{1}H NMR analysis. As this new stereocenter would later be eliminated (*vide infra)*, separation of the stereoisomers was not attempted and the product was used in subsequent steps as a mixture.

Alcohol **12** was treated with 2-methoxypropene and PPTS to generate protected

diol **13** in an 89% yield with a recovery of 11% starting material. The TBS group was then removed with TBAF in THF to give alcohol **14** in a 91% yield.

Scheme 1

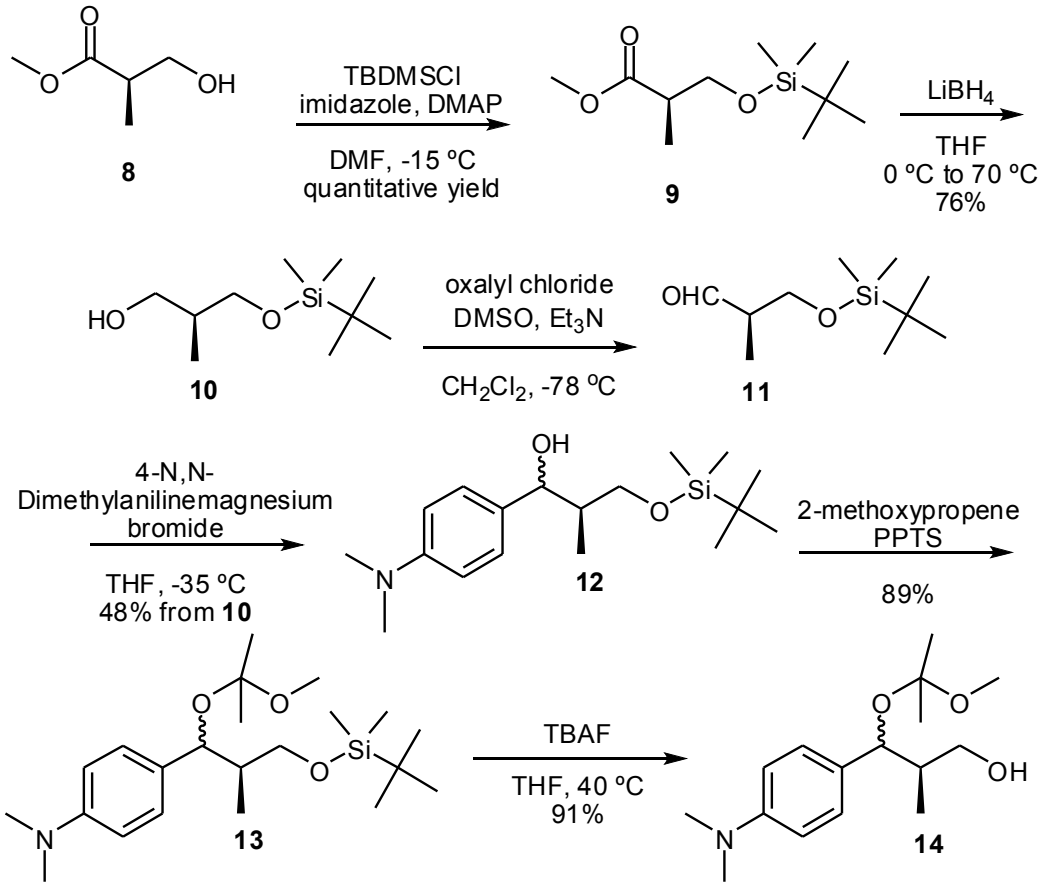

The second portion of the synthesis is presented in Scheme 2. Alcohol **14** was oxidized using Parikh-Doering conditions [68] to form aldehyde **15,** which was used in the next step without purification. This method was chosen instead of the typical Swern conditions based on the findings of Smith *et al.* [69] which showed that this process could result in chlorination at the alpha carbon via an addition to the corresponding enol, which would result in epimerization of the sterocenter. Aldehyde **15** was allowed to react with (1-ethoxycarbonylethylidene) triphenylphosphorane in methylene chloride at reflux for 2 days to produce unsaturated ester **16** in a 76% yield for two steps with recovery of the remaining

24% as unreacted alcohol **14**. Ethyl ester **16** was reduced to alcohol **17** with DIBAL-H in toluene with a 56% yield along with a 41% recovery of ester **16**. Alcohol **17** was then oxidized using Parikh-Doering conditions to form aldehyde **18**, which was immediately treated with (ethoxycarbonyl-methylene) triphenylphosphorane in methylene chloride at reflux for 2 days to provide ester **19** in an 85% yield from alcohol **17**, with an additional 9% recovery of unreacted alcohol **17**.

Scheme 2

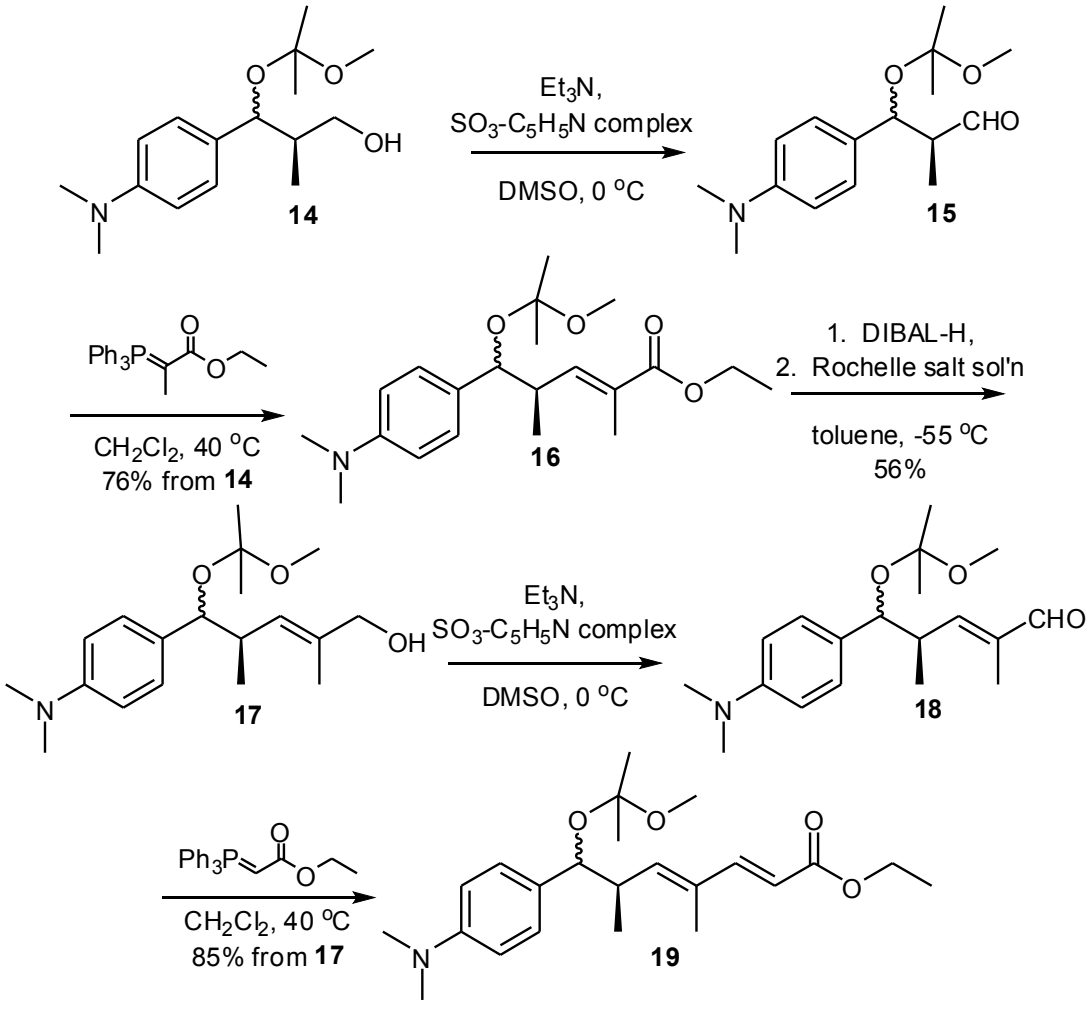

Up to this point, our synthetic route followed Mori and Koseki's synthesis, though we made

several changes, as listed below:

1. We started the initial protection at -15 ºC and used chromatography instead of distillation in purification, giving a quantitative yield (**8** → **9**, Scheme 1).
2. Due to the nearly identical boiling point of the starting material and product (109 ºC vs. 106 ºC) we used chromatography instead of distillation in purification of **10**, which allowed recovery of unreacted starting material.
3. Based on earlier trials (results not shown) we found that the Swern oxidation and resulting Grignard treatment (**10** → **12**, Scheme 1) were more effective if carried out on a smaller scale to more easily control the reaction conditions, and so divided alcohol **10** into smaller portions before starting this reaction.
4. In the deprotection of **14**, we allowed the reaction to go overnight at room temperature rather than stopping it immediately after cooling, which increased our yield from 83.5% to 91%.
5. Due to an eight-fold increase in scale over the published reaction, we increased the reaction time for the Parikh-Doering reaction to form aldehyde **15** to two days, compared to Mori and Koseki's six hours (Scheme 2). While they had a higher yield than we did, we managed to recover all of the unreacted alcohol **14**, which led us to believe that the problem of the lower yield lay in the formation of the aldehyde.
6. Due to a six-fold increase in scale over the published reaction, we increased the reaction time for the anhydrous oxidation to form aldehyde **18** to two days, compared to Mori and Koseki's one day (Scheme 2). This increased our yield from 64% to 85%.

We continued our first synthesis of TSA using the Mori and Koseki route [8], as

presented in Scheme 3. Ethyl ester **19** was treated with lithium hydroxide in methanol for 16 hours at 45 ºC, then the pH of the reaction mixture was lowered to 3 with 1 M aqueous hydrochloric acid to give free acid **20**, which was used in the next step without purification. Acid **20** was then treated with DDQ in 1,4-dioxane to give trichostatin acid (**21)** in a 29% yield. Acid **21** was condensed with hydroxylamine **22**, available in a 10% yield via a two-step sequence from *N*-hydroxyphthalimide (insert, scheme 3) to give the protected hydroxamic acid **23** in a 63% yield. Protected acid **23** was then treated with amberlyst 15 in methanol to give TSA (**1)** in a 46% yield.

Scheme 3

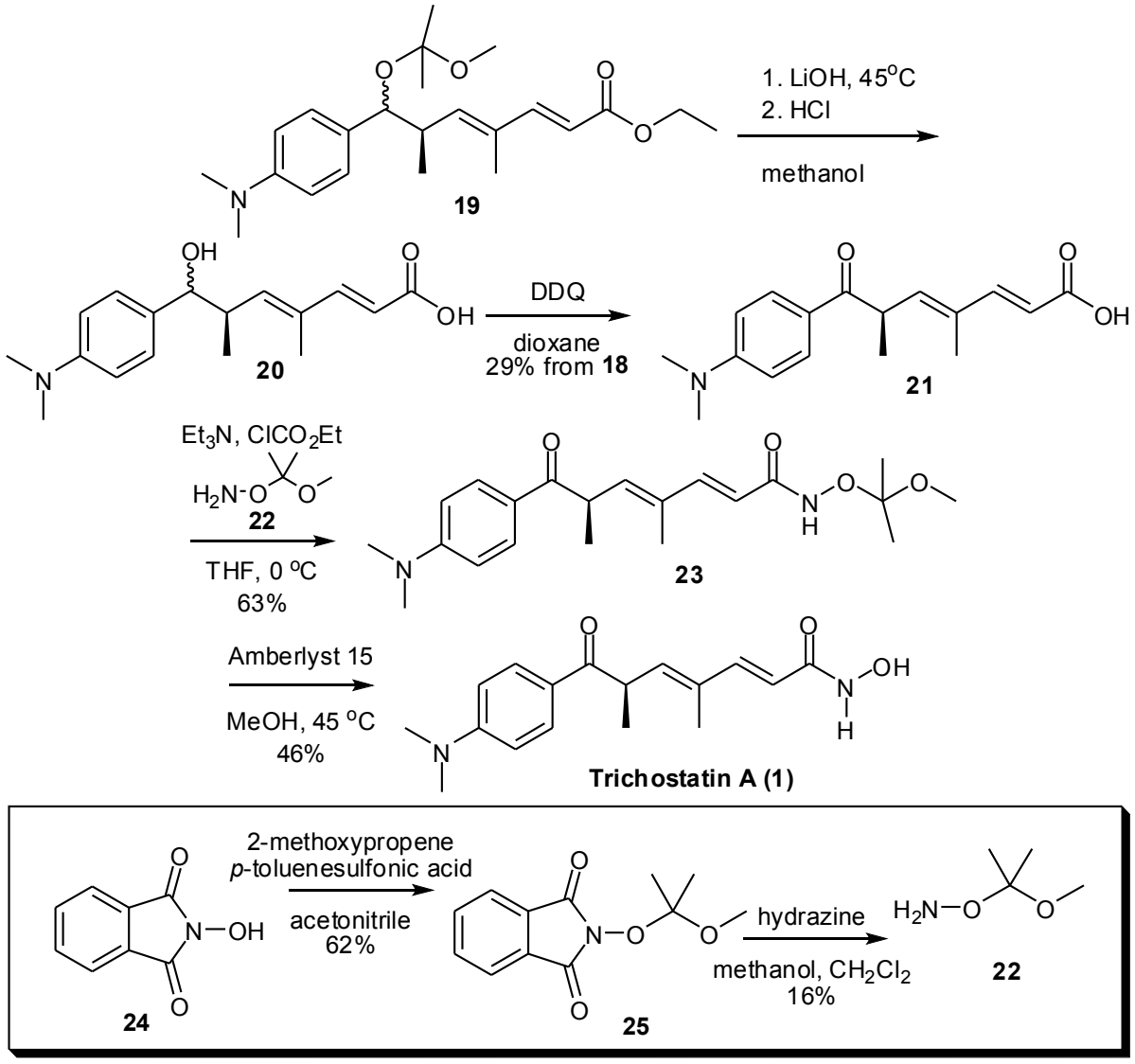

There are two notable problems with the synthesis outlined in Scheme 3. First of all, it is a long process, with some steps, such as the protection of phthalimide **24**, taking several days. Second, it is inefficient, with our overall yield for the last four steps being only 8.4%. However, it is worth noting that this yield is essentially the same as the 9.1% reported by Mori and Koseki [8] for the same four-step sequence. We therefore endeavored to find a shorter, more efficient route to TSA.

Our first alternative ending is described in Scheme 4. As before, ester **19** was treated

with lithium hydroxide and hydrochloric acid in methanol to provide **20**, which was used in the next step without purification. Acid **20** was then treated with DDQ in 1,4-dioxane to produce trichostatin acid (**21**) with a 29% yield for two steps. Acid **21** was then treated with ethyl chloroformate and triethylamine in tetrahydrofuran, followed by hydroxylamine generated *in situ* from potassium hydroxide and hydroxylamine HCl salt in methanol to afford TSA in a 23% yield.

Scheme 4

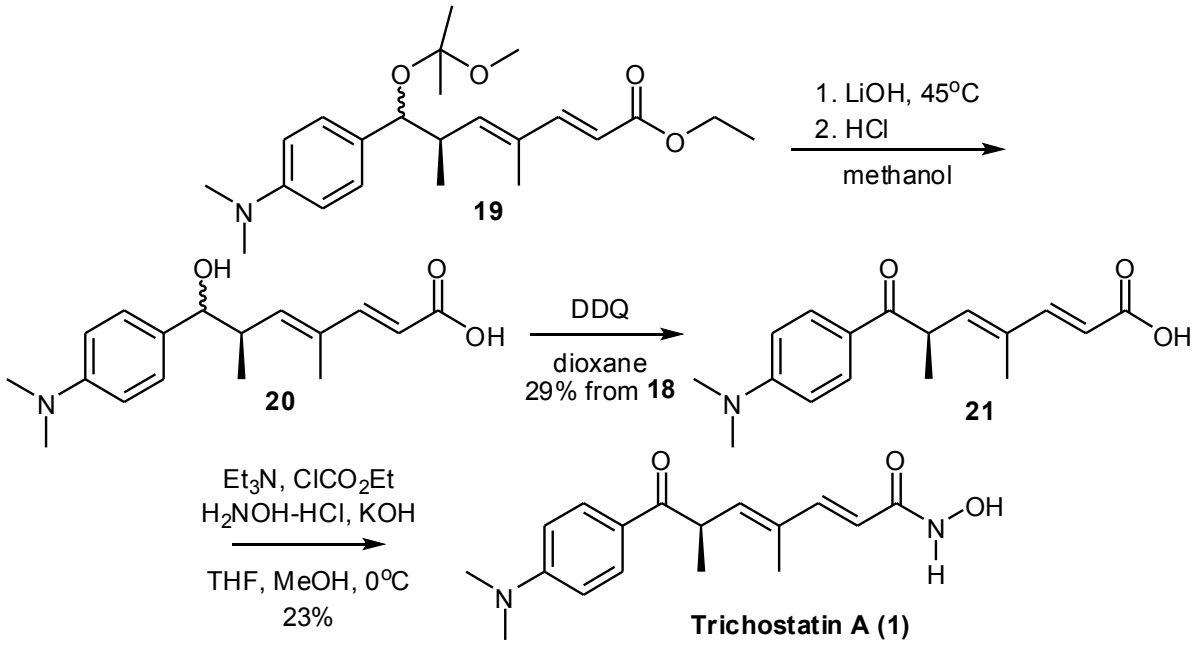

This method decreased the total number of steps for the transformation of ester **19** to TSA **(1)** from four to three, eliminated the need for the synthesis of protected hydroxylamine **22** (cf. scheme 3 insert) and deprotection of the hydroxamic acid in the final step (**23** to **1**, scheme 3), and saved more than a week on the total synthesis. However, it also decreased the yield from **19** to TSA from 8.4% to 6.2%. To address the issue, we decided to change the order of steps to increase the yield on the problematic oxidation and acid deprotection steps.

In our third and final attempt, seen in scheme 5, ketal **19** was cleaved with

hydrochloric acid in THF to give alcohol **26**, while leaving the ethyl ester intact. Alcohol **26** was isolated in 97% yield, with a remaining 2% of ketal **19** recovered in the purification. Finally, alcohol **26** was treated with NH_2OH in methanol to provide the hydroxamic acid **27,** which was used without further purification. Oxidation of hydroxamic acid **27** using DDQ in 1,4 dioxane produced trichostatin A (**1**) with a 58% yield over two steps. In this approach, we originally followed the amidation procedure using potassium hydroxide and the hydroxylamine HCl salt, which gave a yield of 43% over two steps. However, when we used a solution of 50% hydroxylamine in water and potassium hydroxide with **26** in methanol, we improved the yield to 58% over the two steps along with a 33% recovery of ester **26**, which we could not recover in the treatments with hydroxylamine HCl salt.

Scheme 5

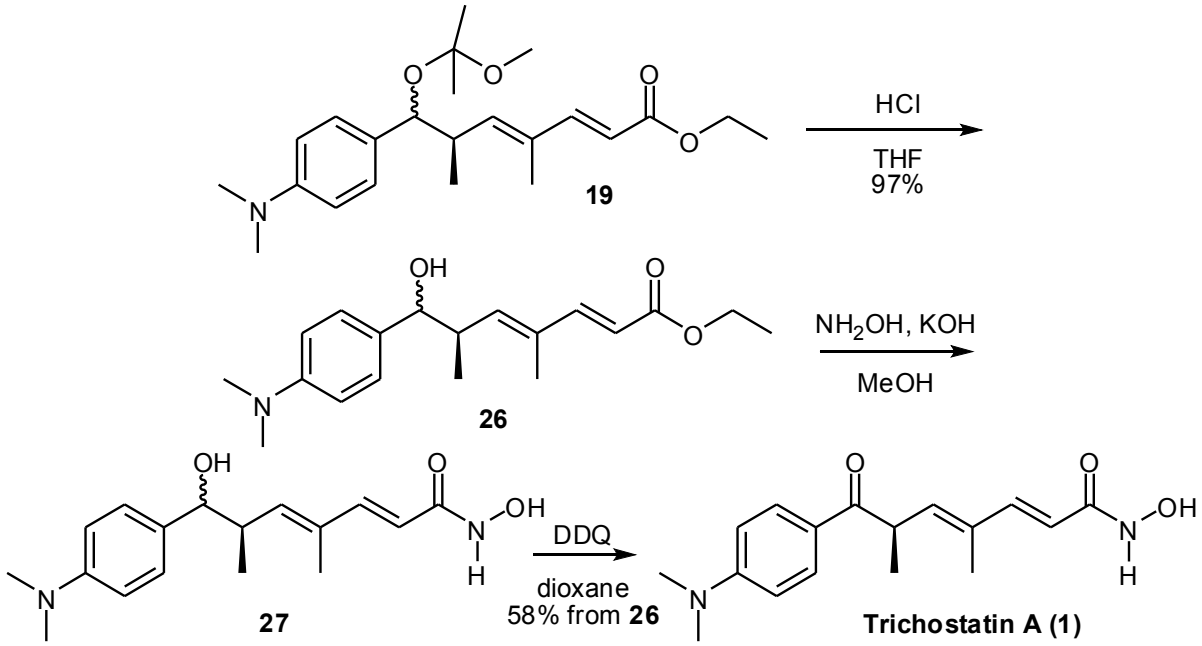

This final route produced TSA in a 56.2% yield from ester **19**, thereby both significantly decreasing the number of steps and greatly increasing the yield when compared to the initial route.

As a result of our research, the total yield of TSA synthesis is 6% over 14 steps. If the recoveries of starting materials are taken into account, this raises the overall yield to 26%.

Chapter III: Summary and Conclusion

The goal of this project was to synthesize TSA and improve upon the existing yield, beginning with a commercially available starting material. The original route by Mori and Koseki featured a longest linear sequence of 15 steps, as well as the necessary two-step synthesis of an intermediate, and had an overall yield of 1.6% (entry 1, table). We were able to accomplish this same synthesis with a comparable yield of 0.9% (entry 2). While our synthesis to **19** had an overall lower yield than that reported by Mori and Koseki (10.7% vs. 17.9%) we were able to recover starting materials from several of the steps, raising our yield on reacted material to 30.4% (entry 5). As a result of our research, we managed to increase the overall yield to the final product from the intermediate **19** from the reported 9.1% (entry 1) to 56.2% (entry 4); if the recovered materials are taken into account, this yield of reacted materials is raised to 85.6% (entry 5). In addition, we managed to substantially reduce the time and decrease the total number of steps in the synthesis from 17 to 14.

Overall, this raises the total yield to 6.0% over 14 steps, or 26% if only considering the reacted materials. As a result of this work, we managed to improve the Mori and Koseki route to TSA and make it more practical and commercially viable for us and more easily available to the research community.

Table 1 Comparison of Yields

Entry	Synthesis	Total # of Steps	**7** to **18 Yield**	**18** to TSA Yield	Overall Yield
1	Mori and Koseki [8]	15	17.90%	9.10%	1.60%
2	Colombo (Scheme 3)	15	10.70%	8.40%	0.90%
3	Colombo (Scheme 4)	14	10.70%	6.20%	0.70%
4	Colombo (Scheme 5)	14	10.70%	56.20%	6.00%
5	Colombo with Recovery of Starting Materials (Scheme 5)	14	30.40%	85.60%	26.00%

Chapter IV: Experimental

General

Anhydrous organic solvents were purchased from Sigma-Aldrich and used without further purification. Reaction progress was monitored by thin-layer chromatography on precoated silica gel GF uniplates from Analchem. Plates were visualized with a 254nm UV lamp and by charring with 50% sulfuric acid. Flash chromatography was performed on 60-63 μM silica gel from Silicycle. Mass spectra were recorded using a Finnigan MAT LCQ. NMR spectra were recorded using a Bruker BB 300 MHz spectrometer. Chemical shifts are reported in ppm (δ) relative to tetramethylsilane, and coupling constants (J) are reported in Hz. Abbreviations for multiplicity are s=singlet d=doublet t=triplet q=quartet dd=doublet of doublets dq=doublet of quartets m=multiplet br=broad.

R-methyl 3-*t*-butyldimethylsilyloxy-2-methylpropionate (9)

R-(-)-3-Hydroxyisobutyric acid methyl ester (21.32 g, 180 mmol), imidazole (31.92 g, 469 mmol) and 4-dimethylaminopyridine (8.81 g, 72.2 mmol) were dissolved in DMF (200 ml) in an oven-dried 500 ml three-neck round bottom flask under nitrogen. The flask was cooled to -15 ºC using an ice/acetone bath, and *t*-butyldimethylsilyl chloride (35.33 g, 235 mmol) was added in three portions each 5 minutes apart, turning the reaction mixture from a clear yellow to a cloudy yellow. The reaction mixture was stirred at -15 ºC for 2 hours, then allowed to warm to room temperature and stir overnight. It was then poured into 200 ml of ice cold water and extracted with ether (1x300 ml, 2x150 ml). The combined organic layers were washed with 30 ml of water and then 40 ml of brine before drying over sodium sulfate, filtration, and concentration in vacuo. The residue was chromatographed over silica using

50:1 hexanes:ethyl acetate to give 43.4 g (>99%) of **9** as a clear colorless oil.

^{1}H NMR ($CDCl_3$) δ 3.75 (1H, dd, J=6.4 and 9.3 Hz) 3.65 (1H, dd, J=6.4 and 9.3 Hz) 3.07 (3H, s) 2.67 (1H, sextet, J=6.4 Hz) 1.15 (3H, d, J=6.9 Hz) 0.90 (9H, s) 0.08 (6H, s).

***R*-2-methyl-3-*t*-butyldimethylsilyloxy-1-propanol (10)**

To an ice-cooled suspension of lithium borohydride (3.49 g, 160 mmol) in THF (110 ml) in a 1000 ml round bottom flask under nitrogen was added a solution of **9** (53.125 g, 228.6 mmol) in THF (270 ml) over 1 hour. After 75 minutes, the flask was equipped with a condenser and heated to reflux (70 ºC) with stirring overnight. The solution was then cooled to 0 ºC and neutralized with a solution of saturated ammonium chloride (60 ml) with stirring until bubbling stopped. The product was then extracted with ether (1x300 ml, 3x100 ml). The combined organics were washed with water (80 ml) and brine (80 ml) before drying over sodium sulfate, filtration, and concentration in vacuo. The residue was chromatographed over silica using a gradient system from 100:1 to 4:1 hexanes:ethyl acetate to give 35.33 g (76%) of **10** as a clear colorless oil, as well as a recovery of 8.68 g (16%) of **9**.

^{1}H NMR ($CDCl_3$) δ 3.64 (4H, m) 1.96 (1H, br) 1.95 (1H, m) 0.90 (9H, s) 0.84 (3H, d, J=6.9 Hz) 0.08 (6H, s).

3-*t*-butyldimethylsilyloxy-1-(4-*N,N*-dimethylaminophenyl)-2-methyl-1-propanol (12)

A 2 M solution of oxalyl chloride in methylene chloride (31.2 ml, 62.4 mmol) was dissolved in methylene chloride (30 ml) in a 250 ml round bottom flask under nitrogen equipped with an addition funnel and cooled to -78 ºC. A solution of DMSO (6.45 g, 82.6 mmol) in methylene chloride (30 ml) was added dropwise and then stirred for 1 hour. A solution of

10 (7.5 g, 36.7 mmol) in methylene chloride (30 ml) was added dropwise, then stirred for 30 minutes. Triethylamine (11.4 g, 112.9 mmol) was then added dropwise over 5 minutes and the reaction mixture was allowed to warm to room temperature. Then 50 ml of water was added and the reaction mixture was extracted with ether (3x150 ml). The combined organics were washed with water (25 ml) and brine (25 ml) before drying over sodium sulfate, filtration, and concentration in vacuo. The residue, **11**, was used crude as a yellow oil and dissolved in THF (45 ml) in a 250 ml round bottom flask under nitrogen and cooled to -35 ºC. 4-*N,N*-Dimethylaminophenyl magnesium bromide (0.5 M in THF, 89.2 mmol) was added dropwise with vigorous stirring, changing from a pale yellow to a deep gold. The solution was stirred for 1 hour at -35 ºC and turned a dark red, then was moved to a -20 ºC environment overnight. The reaction mixture was then brought to room temperature and neutralized with an aqueous solution of saturated ammonium chloride (25 ml) with stirring, turning the reaction mixture black. Water (25 ml) was added and the reaction mixture was extracted with ethyl acetate (1x300 ml, 2x100 ml). The combined organics were washed with water (25 ml) and brine (25 ml), then dried over sodium sulfate, filtered and concentrated in vacuo to yield a black oil. The residue was chromatographed over silica using a gradient system from 40:1 to 20:1 hexanes:ethyl acetate to give 5.71 g (48%) of **12** as a clear pale yellow oil.

^{1}H NMR ($CDCl_3$) δ 7.20 (2H, d, J=6.9 Hz) 6.72 (2H, d, J=6.9 Hz) 4.84 and 4.46 (total 1 H, d, J=7.0 Hz) 3.85-3.55 (2H, m) 2.95 (6H, s) 2.00 (1H, m) 0.94 (9H, s) 0.85 and 0.72 (total 3H, d, J=7.0 Hz) 0.11 and 0.09 (total 6H, s).

3-*t*-butyldimethylsilyloxy-1-(4-*N,N*-dimethylaminophenyl)-1-(2-methoxypropyloxy)-2-methylpropane (13)

To a solution of **12** (28.11 g, 86.8 mmol) in 2-methoxypropene (41.6 ml) in a 125 ml round bottom flask under nitrogen was added PPTS (1.31 g, 5.2 mmol) and the reaction mixture stirred vigorously for 3 hours, turning a dark green. The reaction mixture was neutralized with an aqueous solution of saturated sodium bicarbonate (20 ml) and then extracted with ether (1x300 ml, 3x100 ml). The combined organics were washed with water (50 ml) and brine (50 ml) before drying over sodium sulfate with triethylamine (20 ml), filtration, and concentration in vacuo. The residue was chromatographed over silica using a gradient system from 100:1 to 10:1 hexanes:ethyl acetate with 0.5% triethylamine to give 30.6 g (89%) of **13** as a pale yellow oil, as well as a recovery of 3.11 g (11%) of recovered **12**.

^{1}H NMR ($CDCl_3$) δ 7.15 (2H, d, J=8.7 Hz) 6.69 (2H, d, J=8.7 Hz) 4.69 and 4.58 (total 1H, d, J=6.7 and 10 Hz) 3.55 and 3.18 (total 1H, dd, J=6.7 and 10 Hz) 3.48 (1H, d, J=6.0 Hz) 3.05 and 3.02 (total 3H, s) 2.94 (6H, s) 1.36 and 1.15 (total 6H, s) 0.95 and 0.90 (total 9H, s) 0.80 and 0.67 (total 3H, d, J=6.2 Hz) 0.10 and 0.02 (total 6H, s).

3-(4-*N,N*-dimethylaminophenyl)-3-(2-methoxypropyloxy)-2-methyl-1-propanol (14)

To a solution of **13** (29.798 g, 75.3 mmol) in THF (230 ml) in a 500 ml round bottom flask under nitrogen was added TBAF (1 M solution, 86.6 mmol). The reaction mixture was heated to 40 ºC and stirred for 4 hours, then allowed to cool to room temperature and stirred overnight. The reaction mixture was neutralized with a solution of saturated ammonium chloride (100 ml) and then extracted with ethyl acetate (1x400 ml, 3x250 ml). The combined

organics were washed with water (100 ml) and brine (100 ml) before drying over sodium sulfate with triethylamine (20 ml), filtration, and then concentration in vacuo. The residue was chromatographed over silica using a gradient system from 40:1 to 10:1 hexanes:ethyl acetate with 0.5% triethylamine to give 19.18 g (91%) of **14** as a pale orange oil.

^{1}H NMR ($CDCl_3$) δ 7.16 (2H, d, J=8.7 Hz) 6.68 (2H, d, J=8.7 Hz) 4.79 and 4.46 (total 1H, d, J=6.7 Hz) 3.18 and 3.11 (total 3H, s) 1.41 and 1.13 (total 6H, s) 0.72 and 0.67 (total 3H, d, J=6.2 Hz).

ethyl 2,4-dimethyl-5-(4-*N,N*-dimethylaminophenyl)-5-(2-methoxypropyloxy)-2-pentenoate (16)

A solution of **14** (19.18 g, 68.16 mmol) in DMSO (225 ml) in a 1000 ml round bottom flask was placed under nitrogen and cooled to 0 ºC. Triethylamine (44.1 g, 436 mmol) was then added in one portion with stirring. Sulfur trioxide-pyridine complex (32.55 g, 204.5 mmol) was dissolved in DMSO (150 ml) and added dropwise via syringe over 10 minutes. After stirring 20 minutes, 250 ml of ice cold water was added, and the reaction mixture was extracted with ethyl acetate (1 x 500 ml, 4 x 250 ml). The combined organics were washed with water (2 x 100 ml) and brine (50 ml) before drying over sodium sulfate, filtration, and concentration in vacuo. The residue, **15**, was used crude as a gold oil, and dissolved in methylene chloride (200 ml) in a 500 ml round bottom flask under nitrogen. (1-Ethoxycarbonylethylidene) triphenylphosphorane (61.94 g, 170.4 mmol) was added in one portion. The solution was heated to reflux and stirred for 2 days. The solution was then concentrated in vacuo and then taken up in 50% ethyl acetate in hexane (1 L). The reaction mixture was then filtered, and the precipitate washed with 50% ethyl acetate in hexane (2 x

500 ml.) The combined organics were concentrated in vacuo and chromatographed over silica using a gradient system from 100:1 to 4:1 hexanes:ethyl acetate with 0.5% triethylamine to give 18.92 g (76%) of **16** as a clear yellow oil, as well as a recovery of 4.689 g (24%) of unreacted **14**.

^{1}H NMR ($CDCl_3$) δ 7.15 and 7.12 (total 2 H, d, J=9.3 Hz) 6.68 and 6.65 (total 2 H, d, J=9.3 Hz) 5.80 and 5.74 (total 1 H, d, J=15.0 Hz) 4.51 and 4.42 (total 1H, d, J= 6.0 and 8.0 Hz, respectively) 3.11 and 3.05 (total 3H, s) 2.96 and 2.94 (total 6H, s) 1.88 and 1.79 (total 3 H, d, J=1.9 Hz) 1.38 and 1.31 (total 3H, s) 1.29 and 1.26 (total 3 H, t, J=7.1 Hz) 1.10 and 1.07 (total 3H, s) 1.03 and 0.80 (total 3 H, d, J=7.0 Hz).

2,4-dimethyl-5-(4-*N,N*-dimethylaminophenyl)-5-(2-methoxypropyloxy)-2-penten-1-ol (17)

In a 1000 ml round bottom flask under nitrogen, **16** (21.90g, 60.2 mmol) was dissolved in dry toluene (300 ml) and cooled to -78 ºC. DIBAL-H (1 M in toluene, 144.6 mmol) was added dropwise over 45 minutes, turning the solution red, then stirred for 1 hour. The reaction mixture was quenched with the addition of a saturated Rochelle salt solution (potassium sodium tartrate, 100 ml), turning the solution a pale yellow. The reaction mixture was then allowed to return to room temperature with stirring, then filtered through celite. The precipitate was washed with toluene (500 ml); then the combined organics were washed with saturated Rochelle salt solution (50 ml) before being concentrated in vacuo and chromatographed over silica using a gradient system from 100:1 to 3:1 hexanes:ethyl acetate with 0.5% triethylamine to give 10.86 g (56%) of **17** as a pale yellow oil, as well as a recovery of 8.95 g (41%) of unreacted **16**.

^{1}H NMR ($CDCl_3$) δ 7.12 and 7.10 (total 2 H, d, J=8.5 Hz) 6.67 and 6.63 (total 2 H, d, J=8.5 Hz) 5.19 and 5.10 (total 1 H, d, J=6.5 and 7.5 Hz respectively) 4.42 and 4.40 (total 1H, d, J= 6.5 Hz) 3.99 and 3.88 (total 2H, d, J=5.2 Hz) 3.10 and 3.08 (total 3H, s) 2.96 and 2.93 (total 6H, s) 1.65 and 1.52 (total 3 H, d, J=1.6 Hz) 1.38 and 1.31 (total 3H, s) 1.10 and 1.07 (total 3H, s) 1.00 and 0.80 (total 3 H, d, J=6.7 Hz).

ethyl 4,6-dimethyl-7-(4-*N,N*-dimethylaminophenyl)-7-(2-methoxypropyloxy)-2,4-heptadienoate (19)

A solution of **17** (10.86 g, 33.8 mmol) in DMSO (100 ml) in a 500 ml round bottom flask was placed under nitrogen and cooled to 0 ºC. Triethylamine (21.87 g, 216.3 mmol) was then added in one portion with stirring. Sulfur trioxide-pyridine complex (16.14 g, 101.4 mmol) was dissolved in DMSO (80 ml) and added dropwise via syringe over 10 minutes. After stirring 20 minutes, 125 ml of ice cold water was added, and the reaction mixture was extracted with ethyl acetate (1 x 250 ml, 4 x 125 ml). The combined organics were washed with water (2 x 50 ml) and brine (50 ml) before drying over sodium sulfate, filtration, and then concentration in vacuo. The residue, **18**, was used crude as a gold oil, and dissolved in methylene chloride (200 ml) in a 500 ml round bottom flask under nitrogen. (Ethoxycarbonylmethylene) triphenylphosphorane (41.1 g, 117.9 mmol) was added in one portion. The solution was heated to reflux and stirred for 2 days, turning pink. The solution was then concentrated in vacuo and chromatographed without workup over silica using a gradient system from 100:1 to 3:1 hexanes:ethyl acetate with 0.5% triethylamine to give 11.136 g (85%) of **19** as a clear yellow oil, as well as a recovery of 0.690 g (6.4%) of unreacted **17**.

^{1}H NMR ($CDCl_3$) δ 7.32 and 7.25 (total 1 H, d, J=15.0 Hz) 7.10 and 7.07 (total 2 H, d, J=9.0 Hz) 6.65 and 6.62 (total 2 H, d, J=9.0 Hz) 5.80 and 5.74 (total 1 H, d, J=15.0 Hz) 5.72 and 5.60 (total 1 H, br d, J=10.0 Hz) 4.48 and 4.43 (total 1H, d, J= 6.0 and 6.5 Hz, respectively) 3.76 and 3.74 (total 3H, S) 3.08 and 3.05 (total 3H, s) 2.94 and 2.96 (total 3H, s) 1.78 and 1.69 (total 3H, s) 1.35 and 1.31 (total 3H, s) 1.30 and 1.28 (total 3H, s) 1.00 and 0.83 (total 3 H, d, J=6.5 Hz).

ethyl 4,6-dimethyl-7-(4-*N,N*-dimethylaminophenyl)-7-hydroxy-2,4-heptadienoate (26)

To a solution of **19** (5.547 g, 14.2 mmol) in THF (100 ml) in a 250 ml round bottom flask under nitrogen was added concentrated hydrochloric acid (60 drops, ~370 mmol) dropwise over 5 minutes, changing the reaction mixture from a dark, cloudy yellow to an almost clear pale yellow. After 45 minutes, the reaction mixture was neutralized with an aqueous solution of 1:1 saturated sodium bicarbonate:sodium chloride (120 ml), and the reaction mixture was extracted with ethyl acetate (1x400 ml, 2x200 ml). The combined organics were dried over sodium sulfate, filtered, and concentrated in vacuo. The residue was chromatographed over silica using a gradient system from 20:1 to 7:1 hexanes:ethyl acetate to give 4.365 g (97%) of **26** as a pale yellow oil, as well as a recovery of 0.115 g (2%) of recovered **19**.

^{1}H NMR ($CDCl_3$) δ 7.36 (1 H, dd, J=15.9 and 0.6 Hz), 7.18 (2 H, d, J=8.7 Hz), 6.70 (2 H, d, J=8.7 Hz), 5.86 (1 H, d, J=9.9 Hz), 5.81 (1 H, d, J=15.9 Hz), 4.37 (1 H, d, J=7.5 Hz), 4.20 (2 H, q, J=7.2 Hz), 2.94 (6 H, s), 2.87 (1 H, m), 1.97 (1 H, br), 1.79 (3 H, d, J=1.2 Hz), 1.30 (3 H, t, J=7.2 Hz), 0.85 (3 H, d, J=6.8 Hz).

Trichostatin A (1)

To a stirred solution of **26** (4.2 g, 13.2 mmol) in methanol (50 ml) in a 125 ml round bottom flask under nitrogen was added NH_2OH (50% in water, 8.74 g, 264 mmol) over 5 minutes, followed by KOH (50% in water, 2.23 g, 39.6 mmol). The reaction mixture was allowed to stir for 4 hours, and was then quenched with the addition of aqueous HCl (2N, 30 ml). The reaction mixture was then extracted with ethyl acetate (500 ml, 2 x 200 ml) and dried over sodium sulfate, filtered, and concentrated in vacuo. The resulting product **27** was used crude and dissolved in 1,4-dioxane (100 ml) in a 250 ml round bottom flask under nitrogen. DDQ (3.00 g, 13.2 mmol) was added portionwise every thirty minutes over 3 hours. After another thirty minutes, the reaction mixture was filtered through cotton and washed with 350 ml of dioxane, then concentrated in vacuo to a dark green oil, which was chromatographed over silica using a gradient system from 50:1 to 10:1 methylene chloride:methanol to give 2.32 g of Trichostatin A (58%) as well as 1.4 g of recovered **27** (33%).

^{1}H NMR ($CDCl_3$) δ 7.83 (2H, d, J=9.0 Hz) 7.24 (1H, d, J=15.5 Hz) 6.63 (2H, d, J=9.0 Hz) 5.97 (1H, d, J=9.5 Hz) 5.79 (1H, d, J=15.5 Hz) 4.40 (1H, dq, J=9.5 and 7.0 Hz) 3.08 (6H, s) 1.91 (3H, s) 1.30 (3H, d, J=7.0 Hz) +105º (c=.095, EtOH).

References:

1. Gallinari, P.; Di Marco, S.; Jones, P.; Pallaoro, M.; Steinkühler, C. *Cell Res.* **2007,** *17,* 195–211.
2. Gray, S. G.; Dangond, F. *Epigenetics* **2006,** *1,* 67-75.
3. North, B.; Verdin, E. *Genome Biol.* ***2004,*** *5,* 224.
4. Bieliauskas, A.; Pflum, M. *Chem. Soc. Rev*. **2008,** *37,* 1402–1413.
5. Jones, P.; Steinkühler, C. *Curr. Pharm. Design* **2008,** *14,* 545-561.
6. Gao, L.; Cueto, M.; Asselbergs, F.; Atadja, P. *J. Biol. Chem.* **2002,** *277,* 25748-25755.
7. Tsuji, N.; Kobayashi, N.; Nagashima, K.; Wakisaki, Y.; Koizumi, K. *J. Antibiot.* **1976,** *29,* 1–6.
8. Mori, K.; Koseki, K. *Tetrahedron* **1988,** *44,* 6013-6020.
9. Yoshida, M.; Kijima, M.; Akita, M.; Beppu, T. *J. Biol. Chem.* **1990,** 265, 17174–17179.
10. Codony-Servat, J.; Tapia, M.; Bosch, M,; Oliva, C.; Domingo-Domènech, J.; Mellado, B.; Rolfe, M.; Ross, J.; Gascon, P.; Rovira, A.; Albanell, J. *Mol. Cancer. Ther.* **2006,** *5,* 665–675.
11. Finnin, M. S.; Donigian, J. R.; Cohen, A.; Richon, V. M.; Rifkind, R. A.; Marks, P. A.; Breslow, R.; Pavletich, N. P. *Nature (London)* **1999,** *401,* 188–193.
12. Khan, N.; Jeffers, M.; Kumar, S.; Hackett, C.; Boldog, F.; Khramtsov, N.; Qian, X.; Mills, E.; Berghs, S.; Carey, N.; Finn, P.; Collins, L.; Tumber, A.; Ritchie, J.; Jensen, P.; Lichenstein, H.; Sehested, M. *Biological J.* **2008,** *409,* 581-589.
13. Minucci, S.; Pelicci, P. G. *Nat. Rev. Cancer* **2006,** *6,* 38-51.
14. Garber, K. *Nat. Biotechnol.* **2007,** *25,* 17.

15. Monneret, C. *Eur. J. Med. Chem.* **2005,** *40,* 1–13.

16. Yoshida, M.; Nomura, S.; Beppu, T. *Cancer Res*. **1987,** *47,* 3688–3691.

17. Travers, H.; Spotswood, H. T.; Moss, P. A.; Turner, B. M. *Exp. Cell Res.* **2002,** *280,* 149–158.

18. Taddei, A.; Roche, D.; Bickmore, W.; Almouzni, G. *EMBO Reports* **2005,** *6,* 520-524.

19. Khabele, D.; Son, D. S.; Parl, A. K.; Goldberg, G. L.; Augenlicht, L. H.; Mariadason, J. M.; Rice, V. M. *Cancer Biol. Ther.* **2007,** *6,* 795.

20. Song, J.; Noh, J. H.; Lee, J. H.; Eun, J. W.; Ahn, Y. M.; Kim, S. Y.; Lee, S. H.; Park, W. S.; Yoo, N. J.; Lee, J. Y.; Nam, S. W. *APMIS* **2005,** *113*, 264.

21. Bartling, B.; Hofmann, H. S.; Boettger, T.; Hansen, G.; Burdach, S.; Silber, R. E.; Simm, A. *Lung Cancer* **2005,** *49*, 145.

22. Saji, S.; Kawakami, M.; Hayashi, S.; Yoshida, N.; Hirose, M.; Horiguchi, S. I.; Itoh, A.; Funata, N.; Schreiber, S. L.; Yoshida M.; Toi, M. *Oncogene* **2005**, *24*, 4531.

23. KrennHrubec, K.; Marshall, B. L.; Hedglin, M.; Verdin, E.; Ulrich, S. M. *Bioorg. Med. Chem. Lett.* **2007,** *17,* 2874.

24. Papeleu, P.; Vanhaecke, T.; Elaut, G.; Vinken, M.; Henkens, T.; Snykers, S.; Rogiers, V. *Crit. Rev. Toxicol.* **2005,** *35*, 363-378.

25. Yoshida, M.; Beppu, T. *Exp. Cell Res.* **1988,** *177,* 122–131.

26. Marks, P. A.; Miller, T.; Richon, V. M. *Curr. Opin. Pharmacol*. **2003,** *3*, 344–351.

27. Williams, R.J. *Expert Opin. Invest. Drugs* **2001,** *10,* 1571-1573.

28. Steele, N.; Vidal, L.; Plumb, J.; Attard, G.; Rasmussen, A.; Buhl-Jensen, P.; Brown, R.; Blagden, S.; Evans, J.; de Bono, J. *J. Clin. Oncol*. **2005,** *23,* 3035.

29. Duvic, M.; Vu, J. *Expert Opin. Invest. Drugs* **2007,** *16,* 1111–1120.

30. Olsen, E. A.; Kim, Y. H.; Kuzel, T. M.; Pacheco, T. R.; Foss, F. M.; Parker, S.; Frankel, S. R.; Chen, C.; Ricker, J. L.; Arduino, J. M.; Duvic, M. *J. Clin. Oncol*. **2007,** *25,* 3109–3115.

31. Rasheed, W. K.; Johnstone, R. W.; Prince, R. M. *Expert Opin. Invest. Drugs* **2007,** *16,* 659–678.

32. Piekarz, R. L.; Sackett, D. L.; Bates, S. E. *Cancer J*. **2007,** *13,* 30–39.

33. Marchion, D.; Munster, P. *Expert Rev. Anticancer Ther*. **2007,** *74,* 583–598.

34. Papeleu, P.; Loyer, P.; Vanhaecke, T.; Elaut, G.; Geerts, A.; Guguen-Guillouzo, C.; Rogiers, V. *J. Hepatol.* **2003,** *39,* 374–382.

35. Loyer, P.; Glaise, D.; Cariou, S.; Baffet, G.; Meijer, L.; Guguen-Guillouzo, C. *J. Biol. Chem.* **1994,** *269,* 2491–2500.

36. Vanhaecke, T.; Henkens, T.; Kass, G.; Rogiers, V. *Biochem. Pharmacol.* **2004,** *68,* 753–760.

37. Lee, H.; Lee, S.; Baek, M.; Kim, H. Y.; Jeoung, D. I. *Biotech. Lett.* **2002,** *24,* 377–381.

38. Herold, C.; Ganslmayer, M.; Ocker, M.; Hermann, M.; Geerts, A.; Hahn, E. G.; Schuppan, D. *J. Hepatol.* **2002,** *36,* 233–240.

39. Gray, S. G.; Ekstrom, T. J. *Biochem. Biophys. Res. Commun.* **1998,** *245,* 423–427.

40. Glick, R. D.; Swendeman, S. L.; Coffey, D. C.; Rifkind, R. A.; Marks, P. A.; Richon, V. M.; La Quaglia, M. P. *Cancer Res.* **1999,** *59,* 4392–4399.

41. Schmidt, K.; Gust, R.; Jung, M. *Arch. Pharm. (Weinheim)* **1999,** *332,* 353–357.

42. Butler, L. M.; Agus D. B.; Scher, H. I.; Higgins, B.; Rose, A.; Cordon-Cardo, C.; Thaler. H. T.; Rifkind, R. A.; Marks, P. A.; Richon, V. M. *Cancer Res.* **2000,** *60,*

5165–5170.

43. Zhu, W. G.; Lakshmanan, R. R.; Beal, M. D.; Otterson, G. A. *Cancer Res.* **2001,** *61,* 1327–1333.

44. Inoue, H.; Shiraki, K.; Ohmori, S.; Sakai, T.; Deguchi, M.; Yamanaka, T.; Okano, H.; Nakano, T. *Int. J. Mol. Med.* **2002,** *9,* 521–525.

45. Ranganathan, P.; Rangnekar, V. *Cancer Biol. Ther.* **2005,** *4,* 391-392.

46. Domingo-Domènech, J.; Pippa, R.; Tapia, M,; Gascon, P.; Bachs, O, Bosch, M. *Breast Cancer Res. Treat.* **2008,** *112,* 53-62.

47. Mayo, M. W.; Denlinger, C. E.; Broad, R. M.; Yeung, F.; Reilly, E. T.; Shi, Y.; Jones, D. R. *J. Biol. Chem.* **2003,** *278,* 18980–18989.

48. Sonnemann. J.; Gänge, J.; Kumar, K. S.; Müller, C.; Bader, P.; Beck, J. F. *Invest. New Drugs* **2005,** *23,* 99-109.

49. Romieu, P.; Host, L.; Gobaille, S.; Sandner, G.; Aunis, D.; Zwiller, J. *J. Neurosci.* **2008,** *28,* 9342-9348.

50. Pandey, S.C., Ugale, R., Zhang, H., Tang, L., Prakash, A. *J. Neurosci.* **2008,** *28,* 3729-3737.

51. Berger, S. L. *Curr. Opin. Genet. Dev.* **2002,** *12,* 142–148.

52. Gavin, D.; Kartan, S.; Chase, K.; Grayson, D.; Sharma, R. *Schizophr. Res.* **2008,** *103,* 330–332.

53. Göttlicher, M.; Minucci, S.; Zhu, P.; Krämer, O. H.; Schimpf, A.; Giavara, S.; Sleeman, J. P.; Lo Coco, F.; Nervi, C.; Pelicci, P. G.; Heinzel, T. *EMBO J.* **2001,** *20,* 6969–6978.

54. Sharma, R. P. *Schizophr. Res.* **2005**, *72,* 79–90.

55. Kornek, B.; Lassmann, H. *Brain Pathol.* **1999,** *9,* 651-656.

56. Sercarz, E. E. *J. Autoimmun.* **2000,** *14,* 275-277.

57. Burgoon, M. P., Gilden, D.H., Owens, G. P. *Front. Biosci.* **2004,** *9,* 786-796.

58. Dangond, F.; Hafler, D. A.; Tong, J. K.; Randall, J.; Kojima, R.; Utku, N.; Gullans, S. R. *Biochem. Biophys. Res. Commun.* **1998,** *242,* 648-652.

59. Camelo, S.; Iglesias, A. H.; Hwang, D.; Due, B.; Ryu, H.; Smith, K.; Gray, S. G.; Imitola, J.; Duran, G.; Assaf, B.; Langley, B.; Khoury, S. J.; Stephanopoulos, G.; De Girolami, U.; Ratan, R. R.; Ferrante, R. J.; Dangond, F. *J. Neuroimmunol.* **2005,** *164,* 10-21.

60. Vrbova, G. *Neuromuscul. Disord.* **2008,** *18,* 81-82.

61. Avila, A. M.; Burnett, B. G.; Taye, A. A.; Gabanella, F.; Knight, M.; Hartenstein, P.; Cizman, Z.; Di Prospero, N. A.; Pellizzoni, L.; Fischbeck, K. H.; Sumner, C. *J. Clin. Investig.* **2007,** *117,* 659–671.

62. Kishigami, S.; Mizutani, E.; Ohta, H.; Hikichi, T.; Thuan, N. V.; Wakayama, S.; Bui, H.; Wakayama, T. *Biochem. Biophys. Res. Commun.* **2006,** *340,* 183–189.

63. Li, J.,; Svarcova, O.; Villemoes, K.; Kragh, P.; Schmidt, M.; Bogh, I.; Zhang, Y.; Du, Y.; Lin, L.; Purup, S.; Xue, Q.; Bolund, L.; Yang, H.; Maddox-Hyttel, P.; Vajta, G. *Theriogenology* **2008,** *70,* 800–808.

64. Fleming, I.; Iqbal, J.; Krebs, E. R. *Tetrahedron* **1983,** *39,* 841-846.

65. Zhang, S.; Wenhu, D.; Wang, W. *Adv. Synth. Catal.* **2006,** *348,* 1228-1234.

66. Zhao, X.; Zhang, S.; Duan, W. *Youji Huaxue* **2007**, *27,* 1509-1515

67. Omura, K.; Swern, D. *Tetrahedron* **1978,** *34,* 1651.

68. Parikh, J. R.; Doering, W. von E. *J. Am. Chem. Soc.* **1967,** *89,* 5505.

69. Smith, A.; Leenay, B.T., Liu, H., Nelson, L., and Ball, R. *Tetrahedron Lett.* **1988,** *29,* 49-52.